

# Wideband continuously tunable optical delay line based on wavelength conversion in reflective semiconductor optical amplifiers and fiber dispersion

Zhefeng Hu

Junqiang Sun

Huazhong University of Science and Technology  
College of Optoelectronic Science and  
Engineering

Wuhan National Laboratory for Optoelectronics  
1037 Luoyu Road  
Wuhan, Hubei 430074  
China

E-mail: jqsun@mail.hust.edu.cn

**Abstract.** Two schemes of all-optical tunable delay line are proposed and experimentally demonstrated based on wavelength conversion in reflective semiconductor optical amplifiers (RSOAs) and group-velocity dispersion (GVD) in optical fiber. In the first scheme, large optical delays are shown for a 10 Gbits/s non-return-to-zero (NRZ) signal at short wavelength in the C band. In the second scheme, large optical delays are obtained in the whole C band. The proposed schemes achieve continuously tunable delays with nearly no pulse broadening and very little spectral distortion. © 2009 Society of Photo-Optical Instrumentation Engineers. [DOI: 10.1117/1.3242827]

Subject terms: optical delay line; wavelength conversion; cross-gain modulation; fiber dispersion.

Paper 090114R received Feb. 23, 2009; revised manuscript received Jul. 25, 2009; accepted for publication Aug. 11, 2009; published online Oct. 7, 2009.

## 1 Introduction

Optical devices with tunable pulse delays are of central importance to numerous fields, such as optical coherence tomography,<sup>1</sup> interferometry,<sup>2</sup> and optical communications.<sup>3</sup> In these fields, continuously tunable optical delays over a wide range of delay times are especially expected to provide wide applications and feasibility of the systems. Discretely tunable optical delay lines have been demonstrated by switching pulses out of fiber loops<sup>4</sup> or different lengths of fiber.<sup>5</sup> Alternatively, continuously tunable delays have been reported using optical filters<sup>6</sup> and slow light techniques.<sup>7</sup> But many continuous delay schemes tend to introduce variable chirp or dispersion on the optical data, which should be avoided for optimal system performance.

Recently, a new technique for the generation of continuously tunable delays based on wavelength shifting and group-velocity dispersion (GVD) was demonstrated.<sup>8–10</sup> This approach has several particular advantages, such as wide range of tunable delays, compatibility with short or long pulses, and very little spectral distortion. Especially, our previous scheme based on wavelength conversion in semiconductor optical amplifiers (SOAs) and dispersion in dispersion-compensating fiber (DCF) is very simple without any radio frequency (rf) device, high-power pulsed-pump source or highly nonlinear fiber<sup>10</sup> (HNLF). But this approach also has a significant defect, that the obtainable maximal delay depends on the wavelength of the input signal. In previous work, if the input signal is at a long wavelength in the C band, a large time delay can be achieved when a input probe is chosen at shorter wavelength in the C band. However, if the input signal wavelength is very short

in the C band, the obtainable delay will be very small. To achieve a large time delay, the required probe should be tuned at a much shorter wavelength, which may be far outside the C band and will exceed the tuning range of a C band laser. This becomes a great limit for the applications of the tunable optical delay line in a practical system.

In this paper, we experimentally demonstrate two schemes for all-optical continuously tunable pulse delay generation. In the first one, we improve our previous work, and use two reflective semiconductor optical amplifiers (RSOAs) as wideband rapidly tunable wavelength converters, and a span of single-mode fiber (SMF) as the dispersive medium. A maximal optical delay up to 2600 ps is achieved on a 10 Gbits/s nonreturn-to-zero (NRZ) system, when the input signal is at a very short wavelength in the C band. In the second scheme, we use a system combined of the first scheme and previous work, and achieve large time delays in the whole C band.

## 2 Operation Principle

The controllable delay generator consists of two tunable wavelength converters, a dispersive module, and a dispersion compensator. As shown in Fig. 1(a), in the first case, we turn the wavelength converters on. At the beginning, the wavelength of the signal is converted from  $\lambda_1$  to  $\lambda_2$  by the first wavelength converter. Then we pass the signal  $\lambda_2$  through the dispersive module. After that, the signal wavelength is converted back to  $\lambda_1$  by the second wavelength converter. Due to the difference of the group velocity between  $\lambda_1$  and  $\lambda_2$  caused by the dispersion, a time delay is introduced, which is proportional to the wavelength shift multiplied by the GVD of the dispersive module. The pulse broadening caused by the dispersive module is finally compensated. The time delay can be expressed as

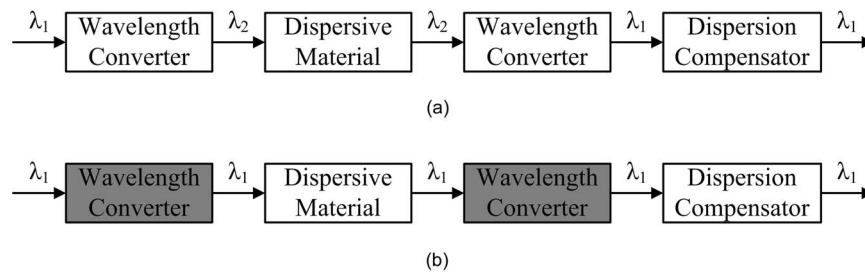


**Fig. 1** Working principles of the time delay generator: (a) time delay generation and (b) working in the undelayed situation.

$$T_d = -DL(\lambda_1 - \lambda_2) \quad (1)$$

where  $T_d$  is time delay,  $D$  is the dispersion coefficient of the dispersive material, and  $L$  is the length of the dispersive material.

In the second case, the wavelength converters are turned off. The signal wavelength is always  $\lambda_1$  in each stage. The output signal is undelayed, as illustrated in Fig. 1(b).

### 3 Experiments

#### 3.1 Large Time Delays for Short Wavelength in the C Band

Figure 2 shows the experimental setup for the first scheme. A continuous wave (cw) at wavelength  $\lambda_1$  is divided into two cws by a 3-dB coupler. One is modulated as the input signal by an electric signal generator (BPG) and a LiNbO<sub>3</sub> modulator. We employ a 10 Gbits/s NRZ pattern of 0100 1110 0011 0010, which repeats per 16 bits, as the input signal. A cw probe  $\lambda_2$  is coupled with the signal into RSOA1. The signal information is modulated onto the probe light with an inverted wave pattern through the effect of cross-gain modulation (XGM) in the RSOA. After filtering out  $\lambda_1$  by a tunable filter (TF1), the probe pulses propagate a 5 km SMF (the total dispersion is 82.8 ps/nm). Then the signal wavelength is converted back to  $\lambda_1$  by RSOA2, also through the effect of XGM, and the wave pattern is inverted back to the same with the input signal. A span of DCF (total dispersion is -84 ps/nm) is used for dispersion compensation. The input power of RSOA1 is 5.1 ( $\lambda_1$ ) and -1.55 dBm ( $\lambda_2$ ), while -3.5 ( $\lambda_1$ ) and 2.7 dBm ( $\lambda_2$ ) at the input of RSOA2. The injected current is 210 mA. An optical spectrum analyzer (OSA, Anritsu MS9710C) with the highest spectral resolution of 0.05 nm is used to monitor

the output spectra, and the optical pulses are observed through a communication signal analyzer (CSA, Tektronix CSA 8000B).

If we disconnect the cw  $\lambda_1$  at point A, and tune all the filters to accept  $\lambda_1$ , the signal pulse train without experiencing wavelength conversion will be obtained. We can observe the time delay through the CSA by comparing this pulse train with that experiencing wavelength conversion.

The waveforms of the pulse trains are shown in Fig. 3. The input signal wavelength is 1532.2 nm, and the probe wavelength is tuned from 1527.6 to 1563.6 nm, which is emitted by a typical C band laser. The corresponding time delays are marked out.

The maximal time delay of 2600 ps can be observed, when the probe wavelength is tuned at 1563.6 nm. While we vary the probe below 1532.2 nm, advancement appears (the sign “-” on time delay denotes pulse advancement). Thus, the scheme achieves continuously tunable optical delays in a wide range by varying the probe wavelength. If the fractional delay is defined as the time delay divided by the pulse width,<sup>11</sup> the maximal fractional delay of 26 is obtained. The scheme obtains large time delay when the input signal is at a short wavelength in C band, without any probe laser far outside the C band.

The optical spectra of the input and output signal are shown in Fig. 4. The central wavelength of the output signal is exactly the same as that of the input signal. Some of the sidebands of the output spectrum are filtered out by the tunable filters. The sidebands can be preserved, when we use wider spectral filters. But this will also preserve the noise in the sidebands.<sup>9</sup> In fact, we find that the section that is filtered out in the sidebands has a negligible influence on the output waveform according to Fig. 3.

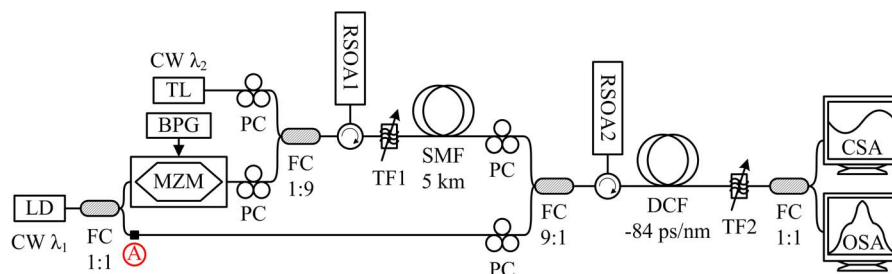


**Fig. 2** Schematic diagram of the continuously tunable optical delay generator: LD, laser diode; TL, tunable laser; BPG, bit pattern generator; FC, fiber coupler; PC, polarization controller; and TF, tunable filter.

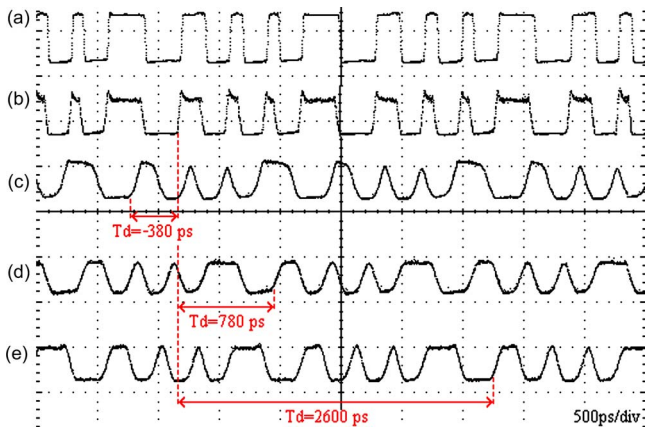


**Fig. 3** Temporal traces for the all-optical delays ( $T_d$ , time delay): (a) input signal, (b) undelayed output, (c) to (e) delayed output, (c)  $\lambda_2=1527.6$  nm, (d)  $\lambda_2=1541.6$  nm, and (e)  $\lambda_2=1563.6$  nm.

Figure 5 illustrates a plot of the relationship between the tunable delay and the probe wavelength. Error bars on the experimental points are smaller than the plotted symbols. It is approximately a linear function with the slope of 82.8 ps/nm, which is equal to the value of total dispersion of the SMF. This slope is opposite to the previous works,<sup>8-10</sup> since the SMF has the opposite dispersive characteristic comparing with DCF.

In the results already mentioned, we fixed the signal wavelength at 1532.2 nm, and tuned the probe wavelength from 1527.6 to 1563.6 nm. Now we vary the signal wavelength in the whole C band, and fix the probe wavelength at 1563.6 nm to measure the obtainable maximal delay for each input signal wavelength. Thus, the dependence of the obtainable maximal delay on the input signal wavelength is denoted in Fig. 6. The complementary effect of the two schemes can be observed clearly in this dependence.

Depicted in Fig. 7 are eye diagrams at different stages with a  $2^{31}-1$ , the pseudorandom binary sequence (PRBS) NRZ signal. We notice that the compensating effect of the

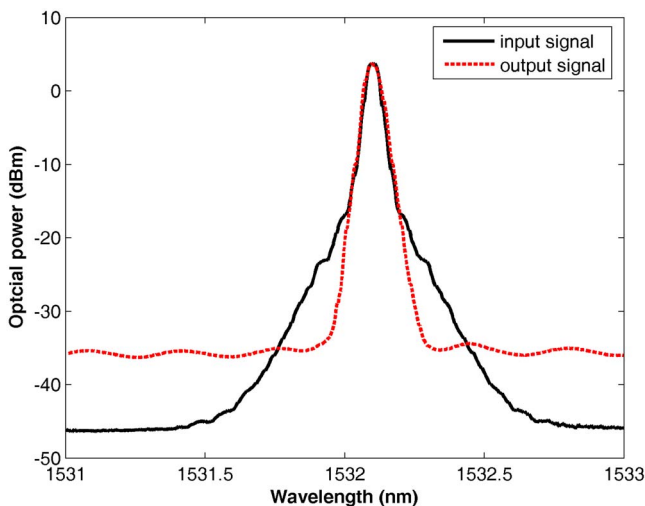


**Fig. 4** Optical spectra of the input (solid line) and output (dash line) signal.

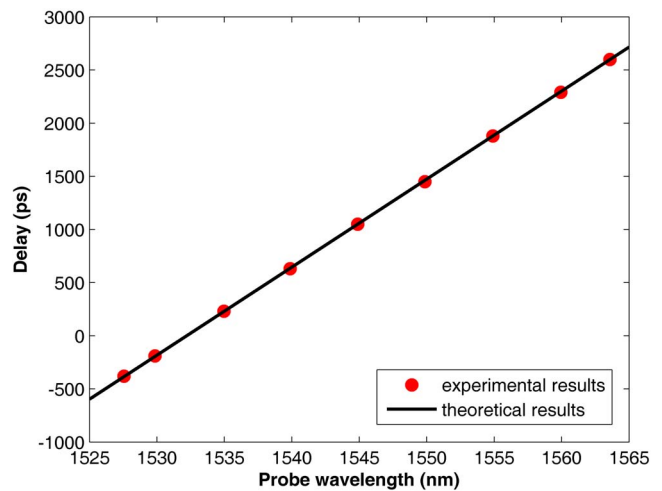


**Fig. 5** Time delay against the probe wavelength ( $\lambda_2$ ).

dispersion-compensation module to the pulse broadening caused by the SMF is not obvious in the waveforms, because the dispersion of the SMF is too small for pulse broadening for a 10 Gbits/s signal. However, from the eye diagrams we know that the signal quality is obviously improved by the DCF in the end. This shows that the effects of tiny pulse broadening and its compensation will be cumulated in the eye diagrams, when a long bit stream is employed. For the consideration of the improvement of the signal quality, the dispersion-compensation module is necessary.

Since the gain peaks of the SOAs which we use in our laboratory are all near 1562 nm, which is far from the wavelength of the input signal, the XGM effect is greatly weakened. Therefore, we employ two RSOAs to increase the effective length of XGM, instead of ordinary transmitting SOAs. The output signal shows an extinction ratio (ER) of 8.6 dB. The RSOAs bring better ER performances than the previous scheme.<sup>10</sup> From Fig. 3, we observe that the signal has some pattern dependent distortions, due to

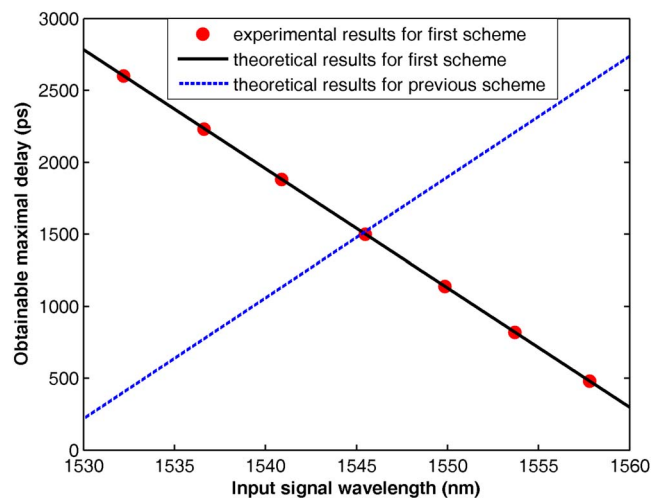


**Fig. 6** Dependence of the obtainable maximal time delay on the input signal wavelength ( $\lambda_1$ ) of the first scheme and previous work.

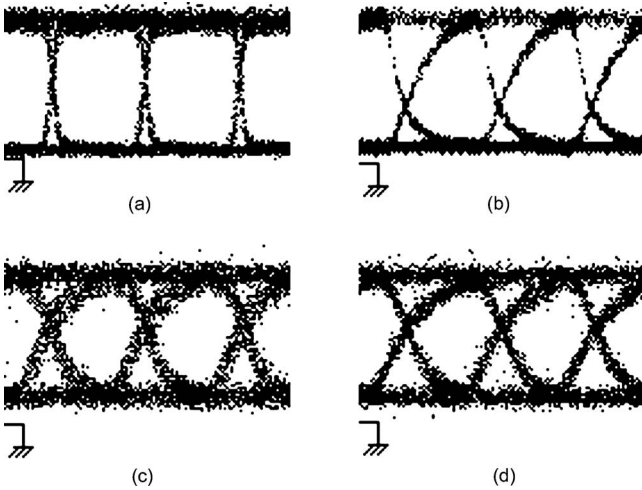


**Fig. 7** Measured eye diagrams: (a) back-to-back, (b) after RSOA1, (c) after RSOA2, without dispersion compensation, and (d) the final output.

the slow recovery of the carrier in RSOA. But the eye diagrams show that the signal quality is still acceptable.

### 3.2 Large Time Delays for the Whole C Band

The scheme already mentioned achieves large time delays at short wavelength in C band. However, the obtainable maximal delay still depends on the wavelength of the input signal. Thus, it can achieve only a very small time delay when the input signal is at long wavelength in C band, without employing any probe laser far outside the C band. But we can use the proposed scheme as the complement to our previous scheme.<sup>10</sup> As such, large time delays can be achieved, whether the input signal is at a long or short wavelength in the C band, by the combination of these two schemes.

As shown in Fig. 8, the combination of the first scheme and our previous work can constitute a complete optical delay generator, which is compatible with input signal at short or long wavelengths in the whole C band. In the combined scheme, the dispersion module and the dispersion-compensation module are modified into the switchable structures between the SMF and the DCF. The optical delay lines (ODLs) are used for signal synchronizing. When the

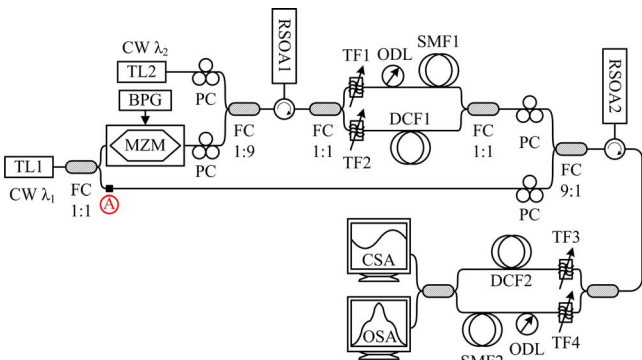


**Fig. 8** Experimental setup of the combined scheme.

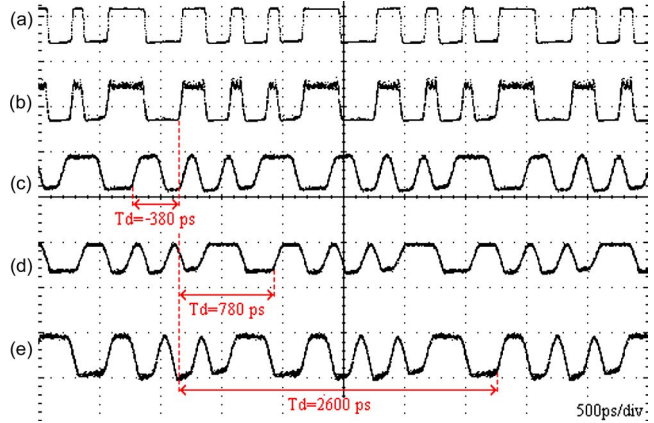


**Fig. 9** Temporal traces of the measured all-optical delays when  $\lambda_1 = 1532.2$  nm: (a) input signal, (b) undelayed output, (c) to (e) delayed output, (c)  $\lambda_2 = 1527.6$  nm, (d)  $\lambda_2 = 1541.6$  nm, and (e)  $\lambda_2 = 1563.6$  nm.

input signal is at short wavelength, TF1 and TF3 are tuned to pass through  $\lambda_1$  and  $\lambda_2$  respectively, and TF2 and TF4 are tuned far from these two wavelengths. Then, SMF1 and DCF2 are used as the dispersion module and the dispersion-compensation module, respectively. If  $\lambda_2$  is tuned at a long wavelength, a large time delay can be achieved. Similarly, when the input signal is at a long wavelength, we should tune TF2 and TF4 to pass through  $\lambda_1$  and  $\lambda_2$ , respectively, and tune TF1 and TF3 far from these two wavelengths, to choose DCF1 and SMF2 as the dispersion module and the dispersion-compensation module, respectively, to obtain a large time delay.

Figures 9 and 10 illustrate the experimental results of tunable delays for  $\lambda_1 = 1532.2$  and  $1557.8$  nm, respectively. The total dispersion of the two spans of SMF are all  $82.8$  ps/nm, and the total dispersion of the two spans of DCF are all  $-84$  ps/nm. TL1 can be varied from  $1532.2$  to  $1557.8$  nm, and TL2 can be tuned from  $1527.6$  to  $1563.6$  nm. A 10-Gbits/s NRZ signal is employed as the input signal.

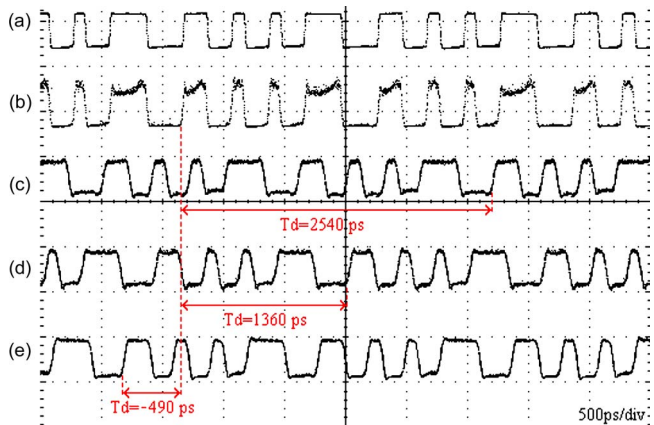


**Fig. 10** Temporal traces of the measured all-optical delays when  $\lambda_1 = 1557.8$  nm: (a) input signal, (b) undelayed output, (c) to (e) delayed output, (c)  $\lambda_2 = 1527.6$  nm, (d)  $\lambda_2 = 1541.6$  nm, and (e)  $\lambda_2 = 1563.6$  nm.

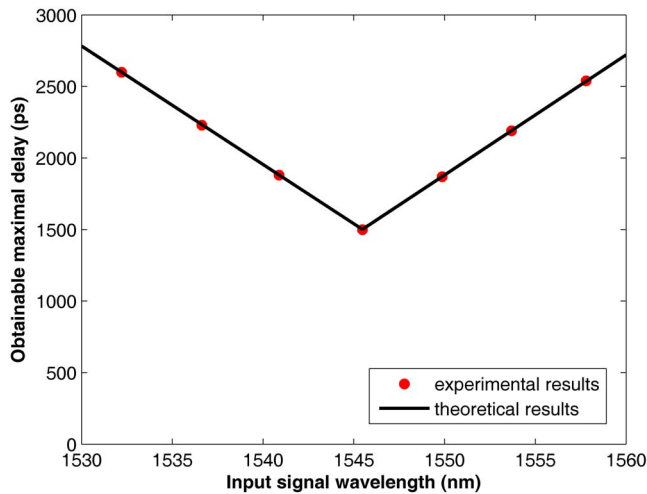


**Fig. 11** Dependence of the obtainable maximal time delay on the input signal wavelength ( $\lambda_1$ ).

Figure 11 denotes the obtainable maximal delay depending on the wavelength of the input signal. The maximal delays from 1500 to 2600 ps can be obtained. The combined scheme achieves large delays in the whole C band. The measured eye diagrams are presented in Fig. 12. An ER of 7.3 dB is shown on the output signal. The ER performance and signal quality is a little worse than the first scheme, because the couplers and the filters bring more power loss before the second RSOA, which will influence the effect of XGM.

#### 4 Discussion

The second scheme shows greater flexibility for a practical optical time delay system, owing to the large time delays over the whole C band. However, the structure is more complicated, and the ER performance and signal quality are worse. Thus, we should choose different schemes according to the application situations. If the input signal is near the

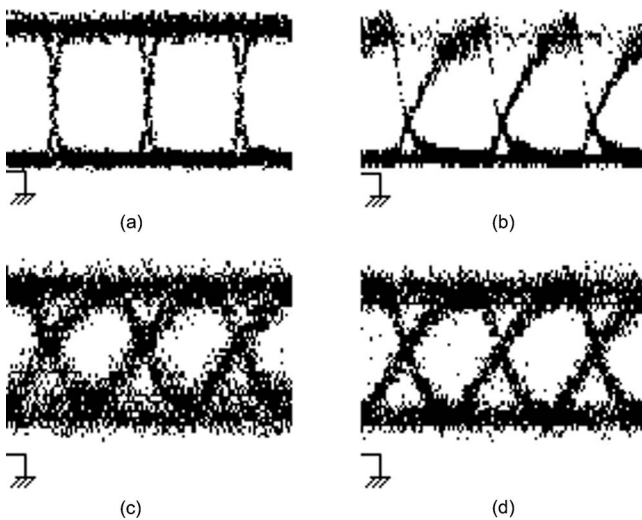


**Fig. 12** Measured eye diagrams: (a) back-to-back, (b) after RSOA1, (c) after RSOA2 without dispersion compensation, and (d) the final output.

long wavelength in the C band, the previous scheme<sup>10</sup> may be a good choice to achieve large tunable time delay. If it is near the short wavelength in the C band, the first scheme can be used. Otherwise, if the input wavelength is varying and unpredictable, the second scheme should be chosen.

#### 5 Conclusion

We demonstrated two continuously variable, all-optical delay generators. In the first scheme, large optical delays were obtained at a short wavelength in C band. The second scheme achieves large optical delays in the whole C band. The proposed all-optical tunable delay lines provide more optional methods for applications in the practical optical communication system in the future.

#### Acknowledgments

The authors would like to thank Jing Li of Yangtze Optical Fiber and Cable Company for providing the SMF and DCF for the experiment. This work was supported by the National Natural Science Foundation of China under Grant No. 60678020 and the Natural Science Foundation of Hubei Province of China under Grant No. 2008CDB313.

#### References

1. C. C. Rosa, J. Rogers, and A. G. Podoleanu, "Fast scanning transmissive delay line for optical coherence tomography," *Opt. Lett.* **30**(24), 3263–3265 (2005).
2. L. Giniunas, R. Danielius, and R. Karkockas, "Scanning delay line with a rotating-parallelogram prism for low-coherence interferometry," *Appl. Opt.*, **38**(34), 7076–7079 (1999).
3. W. Yang, D. Keusters, D. Goswami, and W. S. Warren, "Rapid ultrafine-tunable optical delay line at the 1.55  $\mu\text{m}$  wavelength," *Opt. Lett.* **23**(23), 1843–1845 (1998).
4. K. L. Hall, and K. A. Rauschenbach, "All-optical buffering of 40-Gb/s data packets," *IEEE Photonics Technol. Lett.*, **10**(3), 442–444 (1998).
5. Y. Yeo, J. Yu, and G. Chang, "A dynamically reconfigurable folded-path time delay buffer for optical packet switching," *IEEE Photonics Technol. Lett.* **16**(11), 2559–2561 (2004).
6. G. Lenz, B. J. Eggleton, C. K. Madsen, and R. E. Slusher, "Optical delay lines based on optical filters," *IEEE J. Quantum Electron.*, **37**(4), 525–532 (2001).
7. Y. Okawachi, M. S. Bigelow, J. E. Sharping, Z. Zhu, A. Schweinsberg, D. J. Gauthier, R. W. Boyd, and A. L. Gaeta, "Tunable all-optical delays via Brillouin slow light in an optical fiber," *Phys. Rev. Lett.*, **94**(15), 153902 (2005).
8. J. van Howe and C. Xu, "Ultrafast optical delay line by use of a time-prism pair," *Opt. Lett.* **30**(1), 99–101 (2005).
9. J. E. Sharping, Y. Okawachi, J. van Howe, C. Xu, Y. Wang, A. E. Willner, and A. L. Gaeta, "All-optical, wavelength and bandwidth preserving, pulse delay based on parametric wavelength conversion and dispersion," *Opt. Express*, **13**(20), 7872–7877 (2005).
10. Z. Hu, J. Sun, L. Liu, and J. Wang, "All-optical tunable delay line based on wavelength conversion in semiconductor optical dispersion-compensating fiber," *Appl. Phys. B* **91**, 421–424 (2008).
11. R. W. Boyd, D. J. Gauthier, A. L. Gaeta, and A. E. Willner, "Maximum time delay achievable on propagation through a slow-light medium," *Phys. Rev. A* **71**(2), 023801 (2005).



**Zhefeng Hu** received his BS degree in mechanics engineering in 2002 from Huazhong University of Science and Technology (HUST), where he is currently pursuing his PhD degree in electronics science and technology. His research focuses on all-optical tunable delay, optical buffers, and ultrawideband technology.



**Junqiang Sun** received his PhD degree in electronic physics and optoelectronics from Huazhong University of Science and Technology (HUST) in 1994. From September 2000 to September 2001, he was a research associate with the Department of Electrical and Electronic Engineering, Hongkong University of Science and Technology. From June 2005 to December 2005, he was a research fellow with the school of Information Technology and Engineering, University of Ottawa, Canada. He is now a professor with the College of

Optoelectronic Science and Engineering, HUST. He has published over 100 papers in refereed journals and conference proceeding. His current research interests include all-optical signal processing, all-optical wavelength conversion, fiber lasers and amplifiers, photonic generation of microwave signals, fiber sensors, and optical network technologies.